

Structural aspects of the clustering of curcumin molecules in water. Molecular dynamics computer simulation study

T. Patsahan ¹, O. Pizio ² *

¹ Institute for Condensed Matter Physics of the National Academy of Sciences of Ukraine, 1 Svientsitskii St., 79011 Lviv, Ukraine

² Instituto de Química, Universidad Nacional Autónoma de México, Circuito Exterior, 04510, Cd. Mx., México

Received April 3, 2022, in final form May 10, 2022

We explore clustering of curcumin molecules in water by using the OPLS-UA model for the enol conformer of curcumin (J. Mol. Liq., **223**, 707, 2016) and the SPC-E water model. With this purpose, solutions of 2, 4, 8, 12, 16 and 20 curcumin molecules in 3000 water molecules are studied by using extensive molecular dynamics computer simulations. Radial distributions for the centers of mass of curcumin molecules are evaluated and the running coordination numbers are analyzed. The formation of clusters on time is elucidated. The internal structure of molecules within the cluster is described by using radial distributions of the elements of the curcumin molecule, the orientation descriptors, the order parameter and the radius of gyration. The self-diffusion coefficient of solute molecules in clusters is evaluated. The distribution of water species around clusters is described in detail. A comparison of our findings with computer simulation results of other authors is performed. A possibility to relate predictions of the model with experimental observations is discussed.

Key words: *curcumin, united atom model, molecular dynamics, water, clusters*

1. Introduction

Curcumin is well known as a spice and natural coloring agent. Its pharmacological activity resulting in therapeutic applications were the subject of very many experimental studies during the recent decades, see e.g., [1–5]. Experimental investigations were accompanied by the applications of methods of quantum chemistry in this area of research. However, from a theoretical modelling perspective there is a huge number of variables involved in the experiments. Consequently, there is much room for the development of adequate modelling and verification of theoretical predictions against experimental data [6].

The studies of solutions with curcumin solutes by using computer simulation techniques were initiated quite recently [7–15]. In particular, modelling of the curcumin molecule force field from quantum chemical (QC) calculations, mainly within the B3LYP method and using different versions of Gaussian software, was undertaken in [11, 12, 16, 17]. Justification for the development of the simpler, OPLS-united atom (UA) model (using the OPLS library [18]) for curcumin molecule from our laboratory was provided in [19]. The model was tested in vacuum and in water using classical molecular dynamics simulations [19].

The present work is a continuation of our research of a single curcumin molecule in water, methanol and dimethylsulfoxide in the framework of molecular dynamics computer simulation methodology [19, 20]. In contrast to the previous studies of many authors, we make one important step forward. Namely, we focus on the systems with a larger number of curcumin molecules ($N_{\text{cur}} = 2, 4, 8, 12, 16$ and 20) rather than a monomer. Thus, the effects of interaction between solute molecules compete with solute–solvent

*Corresponding author: oapizio@gmail.com.

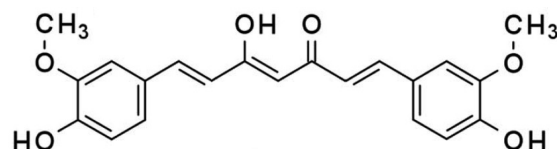


Figure 1. Chemical structure of the enol form of curcumin molecule.

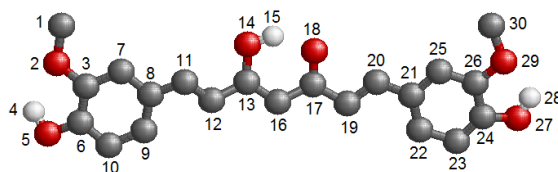


Figure 2. (Colour online) Schematic representation for the united-atom curcumin model with sites numbering. Carbon groups are shown as dark gray spheres, oxygens — as red spheres, hydrogens — as small light-gray spheres.

interaction. This kind of an appealing setup was realized only in [12, 16, 17], up to our best knowledge. It is important to mention that the optimization of the curcumin dimer structure within the QC model was undertaken in [17]. Here, however, we follow the development used in [12]. In close similarity to that work, we focus on the systems with a few curcumin solute molecules in water. It is known that the curcumin molecule is hydrophobic due to the presence of phenyl rings. Hence, the solute is characterized by a very low solubility in water. Water solvent promotes hydrophobic association of curcumin molecules which leads to the formation of clusters. The study of this kind of phenomenon is the principal focus of the present work.

2. Model and simulation details

Molecular dynamics computer simulations of curcumin molecules in water was performed in the isothermal-isobaric (NPT) ensemble at a temperature of 298.15 K and at 1 bar. The GROMACS simulation software [21] version 5.1.4 was used.

Water is described in the framework of popular and well tested SPC-E model [22]. On the other hand, the model developed by using the OPLS-UA force field is used for curcumin molecule [19]. Recently, the model was tested by considering a single curcumin molecule in water, methanol and dimethylsulfoxide [20]. Similarly to our previous investigations, in the present work we restrict our attention to the enol tautomer of curcumin. This structure is dominant in solids and in various solvents, see e.g., [23, 24]. The chemical structure of the molecule is shown in figure 1.

The “ball-and-stick” schematic representation of the molecule was already presented in [19, 20]. Still, we show it here in figure 2, for the sake of convenience of the reader.

All the parameters of the force field can be found in the supporting information file to Ref. [19]. Slight modification of the original model was undertaken, however. In the study of the original model, we observed quite large fluctuations of the bond length between oxygen and hydrogen atoms in the hydroxyl groups H4-O5, H15-O14 as well as in H28-O27. In order to avoid this nonphysical behavior, in the present study these bonds are considered as rigid with the length 0.95 Å and accounted for via constraints. The LINCS algorithm is used.

Technical details of the simulation procedure are as follows. The geometric combination rules were used to determine the parameters for the cross interactions (rule 3 of GROMACS software). To evaluate the Coulomb interaction contributions, the particle mesh Ewald procedure was used (fourth-order spline interpolation and grid spacing for the fast Fourier transform equal to 0.12 nm). The cut-off distance both for Coulomb and Lennard-Jones interactions was chosen equal to 1.1 nm. This choice provides

reasonable computing efficiency and is sufficient to correctly reproduce the properties of interest for all the systems under study. The van der Waals tail correction terms to the energy and pressure were taken into account.

For each system, a periodic cubic simulation box was set up with $N_{\text{wat}} = 3000$ water molecules and N_{cur} curcumin molecules ($N_{\text{cur}} = 2, 4, 8, 12, 16$ and 20). The initial configuration of particles was prepared by placing first the N_{cur} molecules randomly in the simulation box. Next, N_{wat} water molecules were inserted into the box. Each system underwent the energy minimization to remove a possible overlap of atoms in the starting configuration. This was done by applying the steepest descent algorithm. After the minimization procedure, we performed equilibration of each system with the time duration 10 ps at 298.15 K and 1 bar using a small time step 0.1 fs. The Berendsen thermostat with the time coupling constant of 0.1 ps and isotropic Berendsen barostat with the time constant of 2 ps were used. The compressibility parameter was taken equal to $4.5 \cdot 10^{-5} \text{ bar}^{-1}$ (corresponding to the bulk water) in all simulations. It was observed that during equilibration, the curcumin molecules start to assembly and form clusters. At the end of the equilibration run, a few clusters were formed.

After equilibration, the production runs were performed. We used the V-rescale thermostat with the time coupling constant of 0.5 ps and Parrinello-Rahman barostat with the time constant of 2 ps to perform the production runs. The time step was chosen to be 1 fs. The production run was performed in two stages, each of them with time duration of 100 ns. At the first stage, we verify if the curcumin molecules form a cluster and if it behaves as a stable entity. At the second stage, a detailed analysis of the curcumin cluster in aqueous medium was performed. With such time extension of data, we obtain good statistics of events. It is worth mentioning that Hazra et al. [12] studied similar systems by collecting data up to 40 ns only.

3. Results and discussion

3.1. Trends of assembly of curcumin particles in water

To begin with, we extracted the time evolution of the center of mass (COM) of curcumin molecules from the trajectories generated by molecular dynamics for each system under study. Then, the radial distributions for the COM of curcumin molecules were constructed. The functions were obtained at the second stage of each production run and are presented in figure 3, for $N_{\text{cur}} = 8, 12, 16$ and 20 . For $N_{\text{cur}} = 2$ and 4 , the radial distributions are much worse defined because of insufficient statistics. The function $g(r)$ falls to zero at a distance above ≈ 2 nm for all the systems, indicating non-homogeneous distribution of curcumin molecules in the box, or in other words showing that their aggregation occurred. By contrast, the radial distribution function (RDF) of water molecules $g_{\text{OW-OW}}(r)$ (not shown for economy of space) does not exhibit any peculiarity, it behaves as common and tends to unity at large inter-particle separations.

The function $g(r)$ for curcumin molecules has a single maximum in the interval from $r \approx 0.4$ nm to $r \approx 0.5$ nm, if $N_{\text{cur}} = 8, 12, 16$. The maximum slightly shifts to a smaller distance and its height decreases with an increasing number of molecules. Moreover, a shoulder seen at $r \approx 0.8$ nm for $N_{\text{cur}} = 8$ converts into a local minimum at a slightly smaller distance for $N_{\text{cur}} = 12$ and 16 . This behavior reflects the development of a certain structure upon the assembly of curcumin molecules. The width of the distribution upon changes from $N_{\text{cur}} = 8$ to 12 and next to 16 becomes smaller in the interval from 0.3 nm up to $r \approx 1.1$ nm, whereas the outer part, for $r > 1.1$ nm, becomes more diffuse or better say extends to a larger inter-particle separation, if the number of curcumin molecules increases from 8 to 20 . Drastic changes of the shape of $g(r)$ occur, if the number of molecules increases from $N_{\text{cur}} = 16$ to 20 . The first maximum is very narrow for $N_{\text{cur}} = 20$ (its height essentially increases upon the change from $N_{\text{cur}} = 16$ to 20) and the following wavy structure reflects the ordering of curcumin species within the agglomerate.

An additional insight into the trends of the assembly of curcumin particles in water can be obtained from the running coordination numbers defined as follows,

$$n_{\text{cur-cur}}(r) = 4\pi(N_{\text{cur}}/L^3) \int_0^r g(R)R^2 dR, \quad (3.1)$$

where L is the length of the edge of the simulation box. The corresponding curves are given in figure 4. The

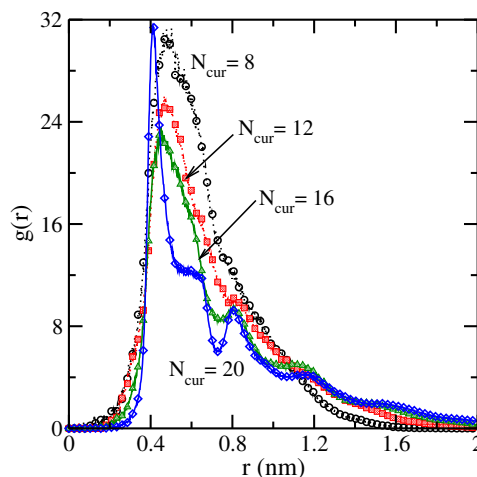


Figure 3. (Colour online) Radial distributions for the center of mass of curcumin molecules in water ($N_w = 3000$) at room temperature.

cyan curve indicates that the size of the agglomerate of curcumin molecules increases non-monotonously. Apparently, the size tends to the saturation value, though in order to prove it, one would need to simulate the systems with a much larger number of particles than we explore in the present work.

It is helpful to put the results shown in figure 3 in the context of findings of other authors. Specifically, Hazra et al. [12] provided the radial distribution of curcumin molecules within their QC model dispersed in the SPC-E water. The bimodal shape of the radial distribution is much stronger pronounced, comparing to our model. The wavy structure was also observed. Unfortunately, neither the number of water molecules was reported nor the value of the chosen mole fraction of curcumin. Just recall, that our plot concerns the effect of augmenting curcumin concentration in the solution.

On the other hand, Bonab et al. [16] used a very similar QC curcumin model as Hazra et al. in combination with the SPC water. The authors restricted to the systems with $N_{\text{cur}} = 2, 3, 4$ and 5 , dispersed in $N_{\text{wat}} \approx 1500$ water molecules in the box. The shape of the radial distribution of curcumin species differs from ours and from Hazra et al. results, cf. figure 3 of [16]. Still, the reported dependence of $g(r)$ on concentration is in agreement with our predictions. Namely, the height of the first maximum decreases with augmenting curcumin concentration (it is located in the interval $r \approx 0.4$ nm to $r \approx 0.5$ nm similarly to our data) and there exists a distance of crossover of the width of the distribution (at a distance we report upon the changes from $N_{\text{cur}} = 8$ to 12).

For the sake of better visualization of the structure that the curcumin molecules attain in water, we present typical snapshots picked up at the end of the second stage of the production run for each system. The plots were prepared by using the VMD software [25]. The 2D plots in the printed version of the manuscript do not permit to appreciate the entire three-dimensional structure, unfortunately.

Still, in the case of a “dimer” ($N_{\text{cur}} = 2$), we observe a pattern describing trends for parallel orientation of molecules, figure 5. Two curcumins are close to each other, water species hardly penetrate the space between much larger molecules. However, one can notice that there are water particles approaching the hydrophilic entities of the curcumin molecules. It is worth mentioning, that the optimized curcumin “dimer” structure of the QC model in the water-ethanol mixture shows a well pronounced parallel motif, cf. table 1 of [17]. Much less order apparently exists in the agglomerate of four curcumin molecules dispersed in water, figure 5. The parallel motif seen in a dimer seems to be perturbed upon aggregation of two more curcumin molecules to the dimer.

If the number of curcumin molecules is larger, $N_{\text{cur}} = 8$ and $N_{\text{cur}} = 12$, one can conclude, from both panels of figure 6, that the trends for parallel ordering are either diminished (left-hand panel of this figure) or enhanced and dominate the structure, as in the right-hand panel. In both cases, it seems that water species are expelled from the interior of agglomerate of curcumin molecules. This issue will be discussed below more in detail.

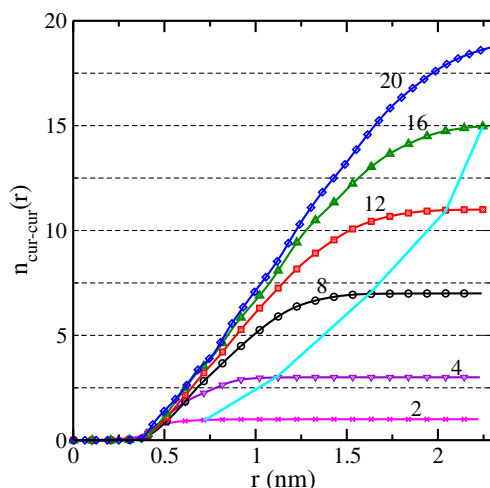


Figure 4. (Colour online) Running coordination number of the COM of curcumin molecules in water ($N_w = 3000$) at room temperature. The number of molecules in each case is marked in the figure. The cyan line joins the points at which the coordination number reaches plateau values with $N_{\text{cur}} - 1$.

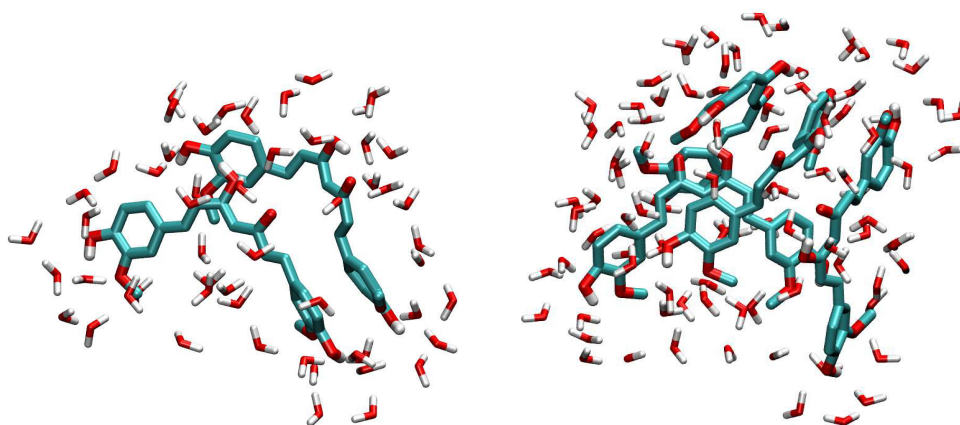


Figure 5. (Colour online) Typical snapshot of the structure attained by 2 and 4 curcumin molecules in water, respectively.

Final snapshots in figure 7 concern the systems with a larger number of curcumin molecules, $N_{\text{cur}} = 16$ and $N_{\text{cur}} = 20$, comparing to previous illustrations. Water particles are not shown in order to make clearer the distribution of solute curcumins. From this visualization, one can get an impression that there exist two parallel motifs, each of them involving a certain number of molecules. However, it seems that these two trends compete or, to put it in other words, two predominant orientations are tilted with respect to each other. We will support this hypothesis in qualitative terms below.

The word cluster in the above part of this section has not been used so far. Now, it is time to do that. We apply the geometric definition for a cluster, in certain similarity to the geometric definition of hydrogen bonds. Namely, taking into account the behavior of the radial distribution of curcumin molecules in water, figure 3, we choose the “cut-off” distance $R_c = 0.75$ nm as a criterion for the cluster definition. This distance approximately coincides with the position of the local minimum observed in the radial distribution of COM of curcumin molecules for the case $N_{\text{cur}} = 16$ and 20 (figure 3). Thus, all the molecules satisfying such geometric criterion along the second stage of the production run are counted as those belonging to a cluster. It is worth mentioning that the radial distributions of curcumin molecules explored with different force field quantitatively differ from the results of the present model,

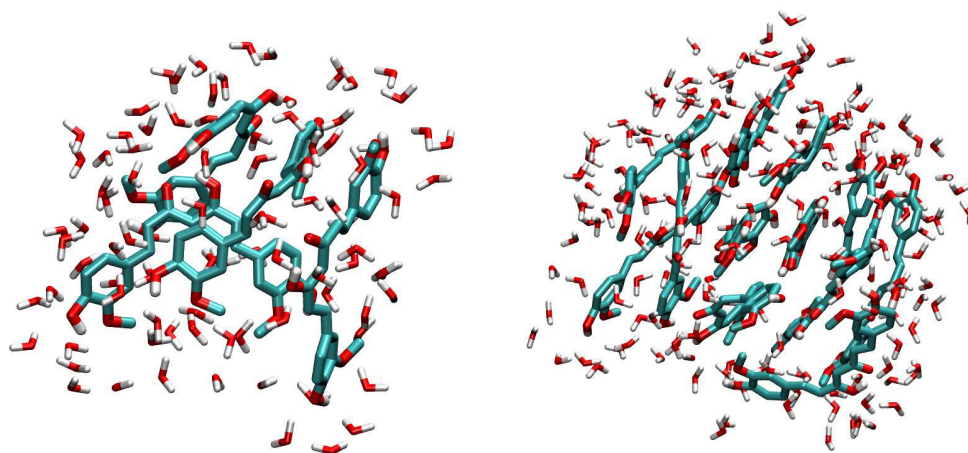


Figure 6. (Colour online) Typical snapshot of the structure attained by 8 and 12 curcumin molecules in water.

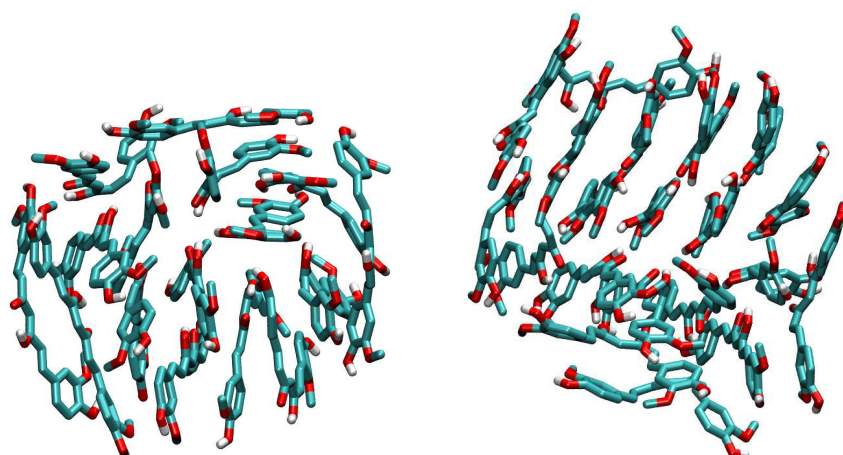


Figure 7. (Colour online) Snapshot of the agglomerates consisting of 16 and 20 curcumin molecules in aqueous medium. The water molecules are not shown to emphasize structural motifs of the distribution of curcumin molecules.

cf. figure 2 of Hazra et al. [12]. In particular, the second maximum, observed for $N_{\text{cur}} = 12$, 16 and 20 for the model in question in figure 3 is small, in contrast to what is reported by Hazra et al. [12] for their QC model. However, these authors used the geometric criterion deduced from the local minimum of the radial distribution as well. In their model $R_c = 0.84$ nm (for $N_{\text{cur}} = 8$ and $N_{\text{cur}} = 12$) and 0.916 for $N_{\text{cur}} = 16$, see [12]. According to our choice of R_c , majority of curcumin molecules for the present model will belong to a cluster, as it follows from the $g(r)$ shape. Only the configurations described by a “long-range” tail of $g(r)$ would permit the molecules out of clusters. By contrast, for the QC model of curcumin in water by Hazra et al., the probability to find the molecules farther than the cluster criterion cut-off is much higher. Therefore, the growth of the clusters on time is expected to be different in the present OPLS model and for the QC model from [12]. Experimental fact is that the curcumin in water-rich solutions has fast aggregation kinetics [17]. However, the experimental time scale and time evolution in computer simulations are two distinct things.

In figure 8 and figure 9 we present the results describing the progress of clusters’ formation during a short period of time from the first stage of production run. It can be seen that the molecules assemble into a cluster within a few nanoseconds, figure 8. However, fluctuations of cluster size persist during the

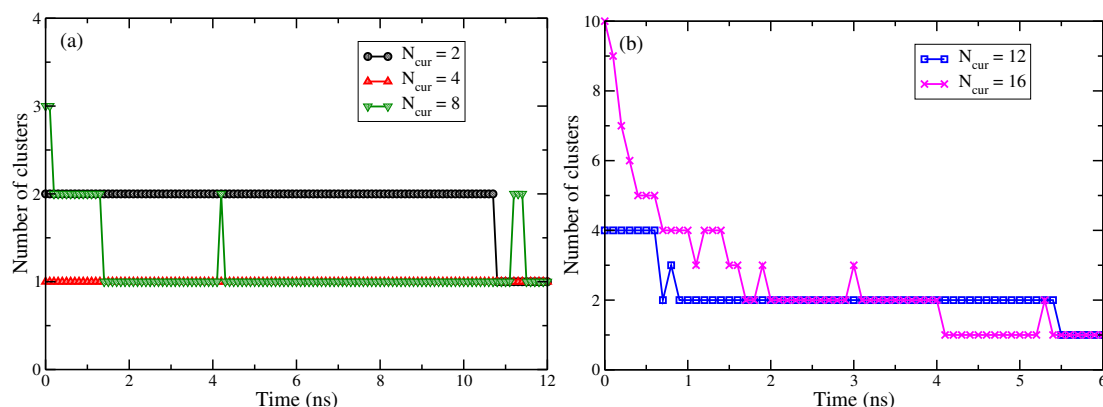


Figure 8. (Colour online) Number of clusters of curcumin molecules at the beginning of the first stage of the production run.

entire trajectory corresponding to the first stage of the production run, figure 9.

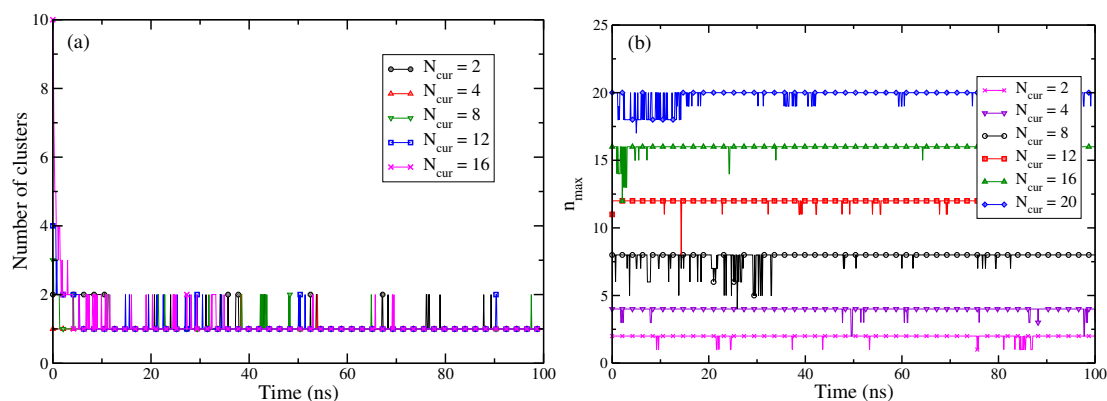


Figure 9. (Colour online) Number of clusters of curcumin molecules (panel a) and the number of molecules in the largest cluster, n_{\max} , dependent on the simulation time along the first stage of the production run.

A detailed description of the formation of cluster for the QC model in water was given in [12]. According to figure 5a of that work, curcumin molecules do not form a single cluster, even at the end of trajectory of 40 ns. It is difficult to prove whether the mechanism of formation of clusters in that work through long-lived intermediates is universal for curcumin in water or whether it is model specific.

3.2. On the internal structure of clusters

In order to analyze the internal structure of clusters formed in each system under study, we pick up all configurations that yield a “complete” cluster, i.e., when the number of molecules in the cluster is equal to N_{cur} during the entire second stage of the production run with the duration of 100 ns.

An overall insight into the radial distribution of curcumin molecules with respect to each other in aqueous medium is given above in figure 3. Now, we turn our attention to the distributions of the structural elements of the curcumin molecules. Trends of the formation of ordered structures can be explored in terms of the radial distributions between the geometric centers of the left-hand (LR) and of the right-hand (RR) phenyl rings, figure 10. In particular, from the LR-LR RDF, panel a of figure 10, we see that there are three maxima corresponding approximately to the distances 0.4, 0.6 and 0.8 nm. The fourth maximum is less pronounced, at $N_{\text{cur}} = 8$ it is just a shoulder. Since the RR-RR counterparts are equivalent to the LR-LR distributions up to statistical inaccuracy, they are not presented.

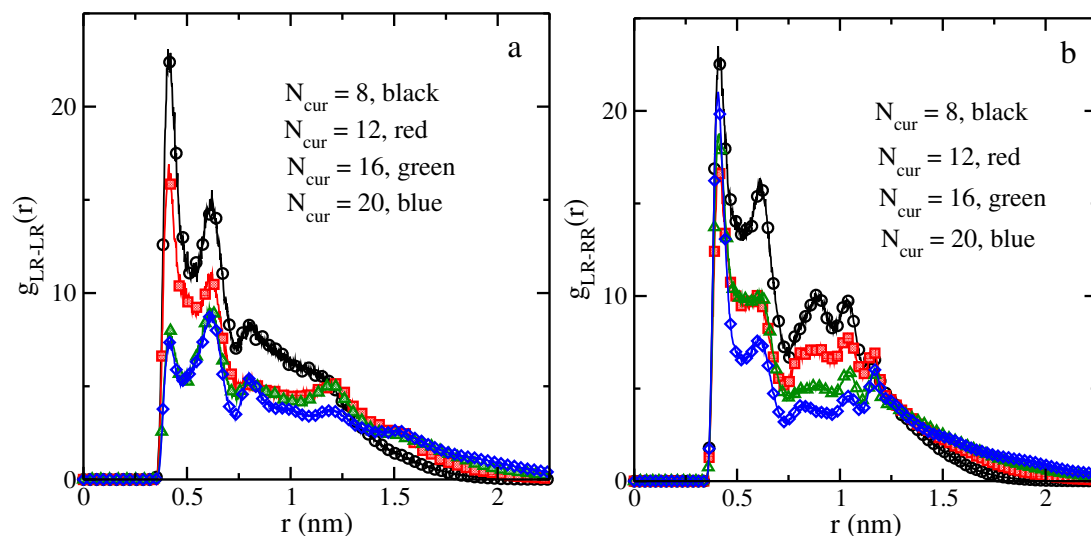


Figure 10. (Colour online) Pair distribution functions between the geometric centers of the left-hand (LR) and of the right-hand (RR) rings of curcumin molecules: LR-LR (panel a) and LR-RR (panel b). In panel b, the intra-molecular peak is also included.

The LR-RR radial distributions, panel b of figure 10, are somewhat different comparing to their LR-LR counterparts. Nevertheless, they have two sharp maxima at 0.4 and 0.6 nm, the third maximum around 0.8 nm is more disperse, comparing to its LR-LR counterpart. The fourth maximum is due to intra-molecular structure of the molecule. These characteristic distances approximately coincide with the distances observed in the curcumin-curcumin COM radial distributions in figure 3. Thus, the behavior of the LR-LR and LR-RR radial distributions can be interpreted as describing parallel and anti-parallel alignment of phenyl rings of curcumin molecules within layer-like structure in the cluster.

The height of the first maximum of the LR-LR and LR-RR distributions is approximately equal if $N_{\text{cur}} = 8$ and 12. However, in larger clusters ($N_{\text{cur}} = 16$ and 20), the first maximum of LR-RR function is much higher, in comparison to LR-LR distribution. Thus, in a smaller cluster, parallel and anti-parallel orientations of phenyl rings of neighboring molecules are approximately “equiprobable” (strictly speaking, these functions do not have probabilistic interpretation). By contrast, in a larger cluster, anti-parallel orientation of phenyl rings of nearest molecules dominates over parallel orientation.

Trends for alignment of curcumin molecules were explored more in detail by calculating the angular probability distribution functions $p(\theta)$ for angles θ between axes of a pair of curcumin molecules (figure 11a). The axis of a molecule is defined as a vector between the geometry center of the left-hand (LR) and the right-hand (RR) phenyl rings. The distribution $p(\theta)$ describes an axial alignment of the curcumin molecules with respect to each other. From the maxima of $p(\theta)$ in figure 11a, one can conclude that curcumin molecules can be oriented not only parallel (or anti-parallel), but also normal to each other. However, the nearest neighbors tend to solely parallel (anti-parallel) ordering, and the perpendicular orientations may correspond to molecules from different domains formed within the cluster, or it can appear due to the perturbations by the proximity of curcumin-water interface.

Another angular probability distribution function $p(\alpha)$ was calculated to analyze the planar alignment of curcumin molecules, where α is an angle between vectors normal to phenyl ring planes (figure 11b). In this case, one can also observe a preferable orientation of the molecular planes, that are either nearly parallel or perpendicular to each other. This behaviour indicates that curcumin molecules tend to form a layered structure in a cluster, although it can be quite distorted due to a small size of clusters.

The parallel and anti-parallel alignment of curcumin molecules in a cluster was discussed by Hazra et al. in [12]. However, the perpendicular orientations of curcumin molecules in the cluster have not been reported since they restricted to the angular probability distribution to the nearest neighbors only.

Trends for axial orientational order of curcumin molecules in a cluster can be captured by using other

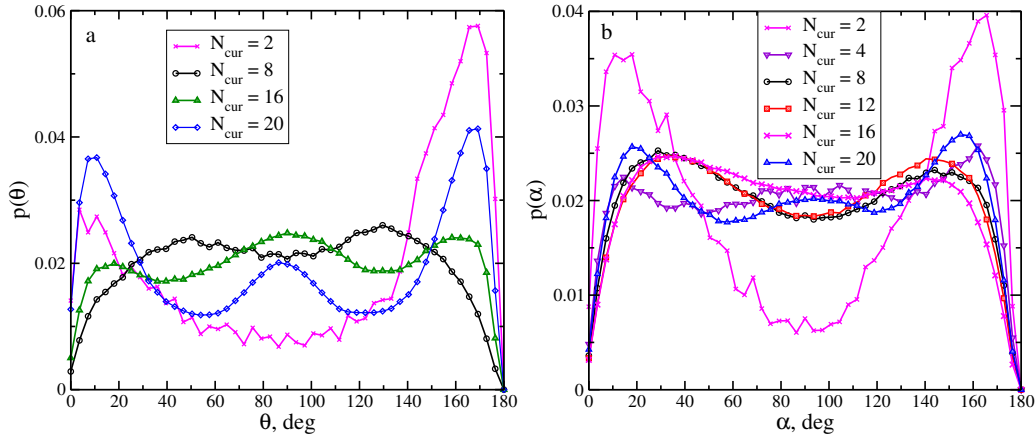


Figure 11. (Colour online) Probability density distribution of the angle between the axes of two curcumin molecules in a cluster of size N_{cur} (panel a). Probability density distribution of the angle between vectors normal to a ring of two curcumin molecules (panel b).

mathematical descriptors. Namely, to inspect this phenomenon, the order parameter, S , of molecules in clusters of sizes $N_{\text{cur}} = 12, 16$ and 20 was calculated from the order parameter tensor,

$$\hat{Q}_{\alpha\beta} = \frac{1}{2N_{\text{cur}}} \sum_{i=1}^{N_{\text{cur}}} (3u_{i,\alpha}u_{i,\beta} - \delta_{\alpha\beta}), \quad \alpha, \beta \in \{x, y, z\}, \quad (3.2)$$

where \mathbf{u}_i is the vector describing the orientation of a molecule i , and δ is the Kroneker symbol. From the diagonalization of tensor \hat{Q} , the uni-axial order parameter $S = \frac{3}{2}\lambda_+$ can be obtained. Here, λ_+ is the largest eigenvalue, and the corresponding eigenvector is the director.

The vector \mathbf{u}_i , to characterize the orientation, is taken along the line connecting geometric centers of the left-hand (LR) and the right-hand (RR) phenyl rings of each of curcumin molecules. Then, the order parameter, S , is calculated at each 10 ps during last 50 ns of the second stage of the production run. This is shown in figure 12a (case $N_{\text{cur}} = 12$ is not presented in order to avoid overload of this panel of the figure). With these data available, the probability density distribution of the order parameter, $p(S)$, is obtained. From figure 12b one can see that molecules in the cluster with $N_{\text{cur}} = 20$ are well uni-axially ordered, the average order parameter is equal to $S \approx 0.65$. The clusters with a smaller number of curcumin molecules $N_{\text{cur}} = 16$ and 12 are characterized by a less pronounced uniaxial motif. Moreover, the average order parameter for $N_{\text{cur}} = 12$ appears to be higher than for $N_{\text{cur}} = 16$, $S \approx 0.5$ and $S \approx 0.4$, respectively.

This behavior can be traced by recalling the non-monotonous changes of the height of the first maximum for curcumin-curcumin RDF in figure 3 with the increasing number of curcumin molecules. Namely, this function indicates the appearance of an additional characteristic length when N_{cur} increases from 12 to 16. In addition, these trends can be elucidated from the snapshots described above. In summary, the cluster growth is not necessarily accompanied by a monotonous growth of the uniaxial order parameter.

Since we consider the clusters consisting of a small number of particles $N_{\text{cur}} \leq 20$, they are not large in space. For example, in the case of $N_{\text{cur}} = 20$, our estimate from the corresponding radial distribution yields a size about 2.2 nm. To get a deeper insight into clusters size change, we calculated the probability distribution functions for the radius of gyration of clusters, figure 13a. The gyration radius is a good descriptor for the cluster compactness.

We observe that the probability density distribution of the gyration radius is unimodal and possesses a certain dispersion. Dispersion of the distribution decreases upon increasing N_{cur} . The dependence of the average radius of gyration on the number of curcumin molecules in a cluster, N_{cur} , is shown in figure 13b. It indicates a monotonous growth of the geometrical size of a cluster with N_{cur} from $R_g = 0.56$ nm up to 1.06 nm. Another estimate for the size of curcumin cluster follows from the radial distribution of water molecules with respect to the COM of the cluster. It is discussed below.

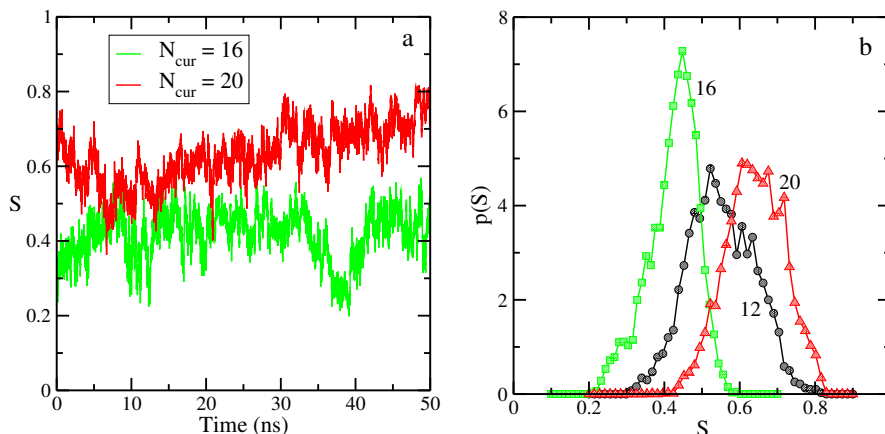


Figure 12. (Colour online) Order parameter of N_{cur} curcumin molecules in a cluster dependent on time (a). Probability density distribution of order parameter of N_{cur} curcumin molecules in a cluster (b).

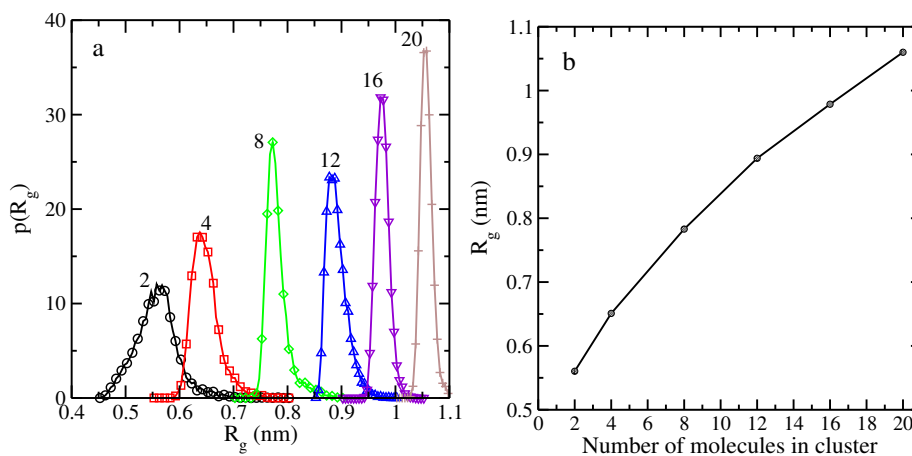


Figure 13. (Colour online) Probability density distribution of R_g of the largest cluster of curcumin molecules (left-hand panel). Radius of gyration, R_g , as a function of the number of curcumin molecules N_{cur} (right-hand panel).

3.3. On the self-diffusion coefficient of curcumin species

Obviously, the dynamic properties of curcumin cluster are affected by its size. One of the methods to obtain the self-diffusion coefficients is from the mean square displacement of species. The mean-square displacement (MSD) is obtained from the simulation trajectories during the second stage of production runs.

In figure 14a, we show the MSD functions of the COM for curcumin cluster of different sizes N_{cur} . It is worth noting that after 20 ns these functions behave linearly with time. Therefore, the time interval of 20 – 40 ns was used to estimate the self-diffusion coefficients of clusters, D_{cur} , from the presented MSD functions by using the Einstein relation,

$$D_i = \frac{1}{6} \lim_{t \rightarrow \infty} \frac{d}{dt} |\mathbf{r}_i(\tau + t) - \mathbf{r}_i(\tau)|^2, \quad (3.3)$$

where i refers to the COM of a curcumin molecule belonging to a cluster, and τ is the time origin.

One can see that the self-diffusion for $N_{\text{cur}} = 2$ is somewhat smaller ($0.378 \cdot 10^{-5} \text{ cm}^2/\text{s}$) than for the case of single curcumin molecule in water ($0.423 \cdot 10^{-5} \text{ cm}^2/\text{s}$) obtained by us earlier in [20].

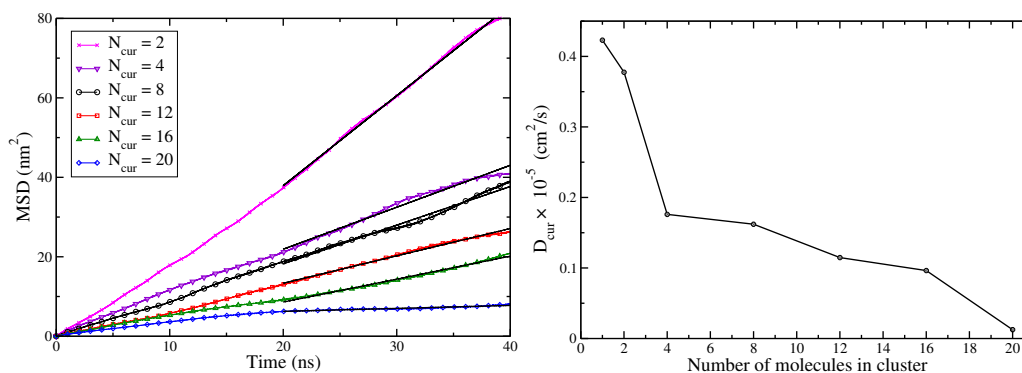


Figure 14. (Colour online) Mean-square displacement of the center of mass of a curcumin molecule belonging to a cluster with a size N_{cur} (left-hand panel). Self-diffusion coefficient of a curcumin molecule belonging to a cluster as a function of the number of molecules in the cluster N_{cur} (right-hand panel).

However, it drastically decreases to $D_{\text{cur}} = 0.176 \cdot 10^{-5} \text{ cm}^2/\text{s}$ for $N_{\text{cur}} = 4$, afterwards it falls down to $D_{\text{cur}} = 0.096349 \cdot 10^{-5} \text{ cm}^2/\text{s}$ for $N_{\text{cur}} = 16$. Finally, the self-diffusion coefficient reaches a very small value $D_{\text{cur}} = 0.012496 \cdot 10^{-5} \text{ cm}^2/\text{s}$ for $N_{\text{cur}} = 20$, figure 14b. Apparently, a single curcumin molecule and the “dimer” aggregate find enough space for translational motion in water. By contrast, the translation motion of a molecule belonging to a larger cluster becomes essentially hindered. Finally, in a big cluster, the curcumin molecules become almost “frozen”.

Alternatively, it would be of interest to perform calculations of dynamical properties by using the velocity auto-correlation functions (VACFs). This method would permit to obtain the self-diffusion coefficient as well, and to compare the results with the predictions from the MSD. Most importantly, the VACF calculations provide an ampler set of dynamic properties, such as relaxation times and vibrational spectra. These issues will be discussed in a separate work.

3.4. On the hydration of clusters

One of important aspects of the self-assembly of curcumin particles in water is the hydration of clusters. Cluster formation intuitively should be accompanied by the process in which the water molecules are expelled from the cluster body. On the other hand, the cluster surface formed due to self-assembly should be geometrically and energetically heterogeneous. Thus, the structure of such an interface can be quite complex.

In order to get insight into this kind of interfaces, we first construct a radial distribution of water oxygens around the COM of a cluster of curcumin species. As expected, the water molecules are expelled from the cluster body, figure 15. The functions constructed for systems with a different number of curcumins saturate to unity at a distance dependent on N_{cur} . The width of the interface is diffuse indicating a certain degree of permeation of water molecules into a cluster. Moreover, it is difficult to unequivocally establish the trends of changes of the width of this interface. Apparently, in all the cases, rate of changes of this function is similar, though in the case of a larger cluster. Namely, if N_{cur} changes from 16 to 20, the interface width becomes wider.

In order to get insights into the structure of the interface formed upon the assembly of curcumin species, we constructed a set of radial distribution functions for different atoms of the curcumin molecule and water. They are shown in figure 16 and figure 17. First, we picked up the oxygen and hydrogen atoms, O14 and H15 respectively, of a curcumin molecule as a reference and built up the radial distribution of atoms of water molecules. The corresponding functions, for e.g., $N_{\text{cur}} = 16$, reach saturation for r larger than $\approx 1.6 \text{ nm}$, figure 16. This estimate agrees with the observations coming from $g(r)$ in the previous figure 15. This behavior could be anticipated, because O14 and H15 atoms are close to the COM of a molecule and presumably are situated in the cluster interior. It is worth mentioning that a single curcumin molecule is quite hydrophobic, i.e., water molecules do not like to approach O14 and H15, as it follows

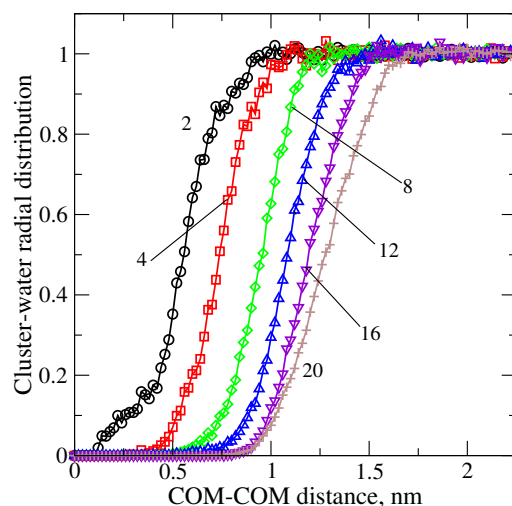


Figure 15. (Colour online) Radial distribution function of water molecules around a curcumin cluster with respect to its COM.

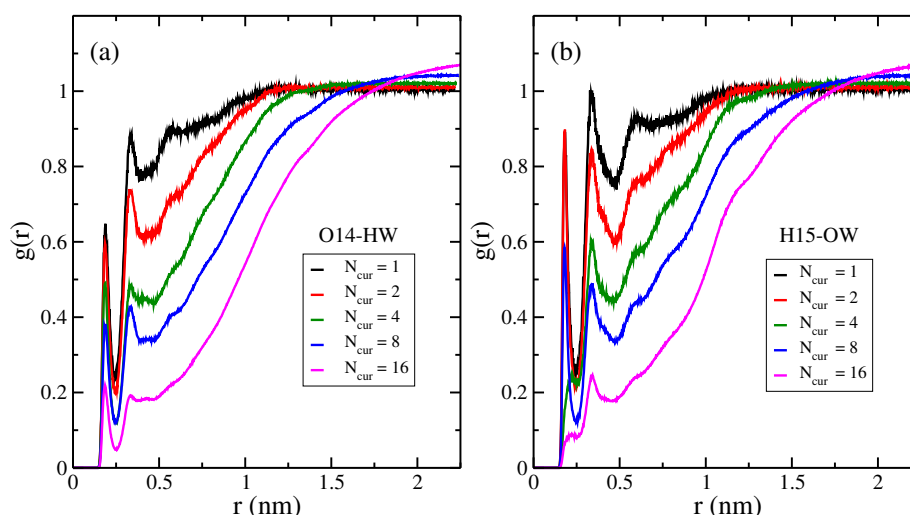


Figure 16. (Colour online) Pair distribution function O14-HW (left-hand panel) and H15-OW (right-hand panel).

from the black curves in figure 16. However, as a manifestation of cooperativity in the case of even a small cluster, this fragment of a curcumin molecule becomes much stronger hydrophobic.

Next, we picked up oxygen and hydrogen atoms, O5 and H4 respectively, of a curcumin molecule and plot radial distribution of atoms of water molecules, figure 17. These atoms are far from the center of mass of a single curcumin molecule. Moreover, according to the snapshots and other structural indicators discussed above, these atoms should be situated on the external surface of a cluster. Consequently, we observe that the cooperative effect of self-assembly of curcumins into a cluster is not very strong at small inter-particle separations. A certain amount of water molecules prefers to locate quite close to O5 and H4 even if the cluster is formed, quite similarly to a single curcumin molecule in water. Moreover, the shape of the functions with multiple peaks in figure 17 indicate the existence of water structure close to O5 and H4. Thus, on average the degree of hydrophobicity of these fragments of curcumin molecules is much less pronounced, in comparison to the fragments involving O14 and H15.

In addition, we explored the distribution of water close to the carbon groups of the phenyl rings. The

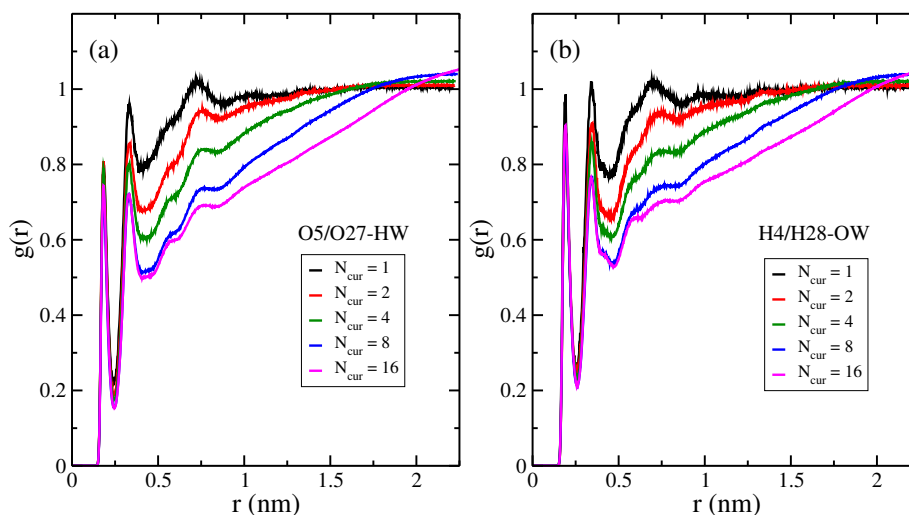


Figure 17. (Colour online) Pair distribution function O5/O27-HW (panel a) and H4/H28-OW (panel b).

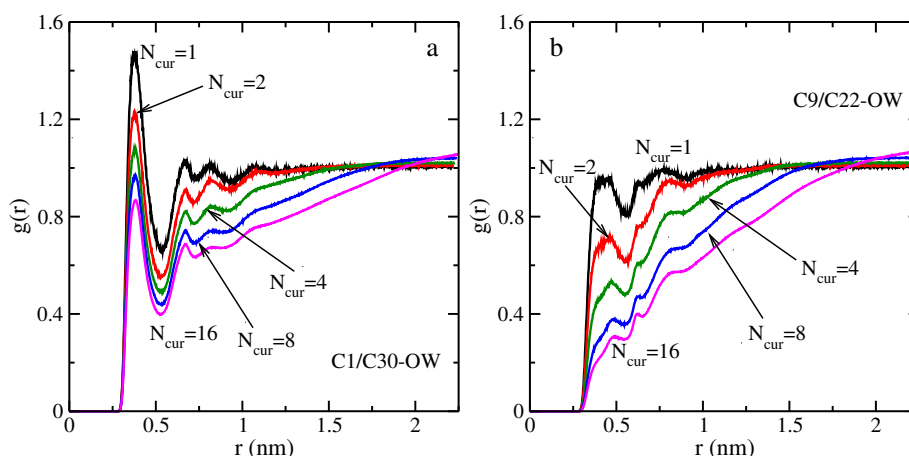


Figure 18. (Colour online) Pair distribution function C1/C30-OW (panel a) and C9/C22-OW (panel b).

results are shown in figure 18. Apparently, this distribution of water molecules is strongly affected by the formation of a cluster. The entire curve yielding this kind of $g(r)$ moves down strongly, if the cluster size increases, indicating cooperative hydrophobicity. The shape of radial distribution in the present case (for a large cluster) is quite similar to what we observed in figure 17. However, the water structure close to C1 (or equivalently close to C30) is less pronounced or smoother, in comparison to the structure close to O5.

In summary, less hydrophobicity of the surface of a cluster for the systems of this study can be attributed to O5, H4, or equivalently to O27, H28 fragments of the curcumin molecules.

4. Summary and conclusions

To conclude, in this work we have presented a very detailed description of the properties of solutions consisting of a different number of curcumin molecule (from 2 to 16) in 3000 molecules of water. The home-made, non-polarizable OPLS-UA model for curcumin molecule was used. On the other hand, water is considered by using the SPC-E model. Geometric combination rules were applied. The simulations were

performed by using isobaric-isothermal conditions. Our principal issue was in obtaining and analysing the structural aspects of self-assembly of curcumin molecules in an aqueous medium.

General trends of our findings are in a qualitative agreement with the recent similar kind of systems performed in the laboratory of Bagchi [12] by using a different model of curcumin molecules. However, we offer a wider set of properties in comparison to that work. Namely, we analyzed various orientational descriptors for the distribution of curcumins in a cluster, the radius of gyration of a cluster, order parameter and diffusion coefficient. The cluster-water interface is characterized by several radial distribution functions that indicate its geometric and energetic heterogeneity and an overall hydrophobicity.

Still, similarly to [12], we were unable to find an appropriate experimental setup to verify our predictions from computer simulations versus experiment. Apparently, this can be done in future, by adding a certain amount of a co-solvent that should lead to disaggregation of clusters. Specifically, the systems consisting of curcumin species in water-ethanol solvent of variable composition were studied very recently using molecular dynamics computer simulations and experimental methods [17]. The study made use of determining the so-called critical water aggregation percentage (CWAP) to delimit the monomeric form of curcumin species from aggregates. Experimentally, the CWAP, i.e., the percentage of water below which curcumin is in its monomeric form predominantly, was evaluated from the analyses of the effect of electronic absorption spectra and of fluorescence emission spectra on the solvent composition, see e.g., the discussion of figures 2 and 3 of [17]. This quantity may provide good test of the quality of the curcumin model of the present study.

Several interesting and important issues, even within the present stage of modelling, require additional investigation. Namely, a more detailed description of the solute - solvent interface would be desirable in perspective. The properties of a solvent and of a co-solvent, if present, around a biomolecule determine its conformations and affect trends to form clusters. Evidently, the “direct” interaction between such complex solutes is of importance in the latter aspect as well. Moreover, at the level of a more sophisticated modelling, one may attempt to elucidate the role of the polarizability of solute molecules. At present, for the system of our interest, it is difficult to profoundly discern and analyze each type of the effects. Interesting discussion of some of these issues for a simpler, dimethylsulfoxide-water solutions was given in [26].

Concerning the formation of clusters of curcumin molecules, one may attempt to take advantage of the system with two curcumin molecules dispersed in a solvent. Then, along the line of previous studies of simpler molecular fluids, one may focus on the evaluation of the potential of the mean force (PMF). The software of the present study permits to obtain the PMF for the center of mass of curcumin species. Then, the second virial coefficient at a given thermodynamic conditions can be calculated. The molecular clustering phenomena can be analyzed in terms of the virial coefficients, as it was proposed originally in [27] and implemented for water in the laboratory of Kofke [28, 29]. This kind of methodology is of interest in a wider context and for the systems of the present work as well, see e.g., [30]. Some of these issues are under study in our research groups.

Acknowledgement

O.P. is grateful to M. Aguilar for technical support of this work at the Institute of Chemistry of UNAM. Fruitful discussions with Dr. Manuel Soriano at the early stage of this project are gratefully acknowledged. T.P. acknowledges allocation of computer time at the cluster of ICMP of the National Academy of Science of Ukraine and Ukrainian National Grid.

References

1. Ghosh S., Banerjee S., Sil P. C., *Food Chem. Toxicol.*, 2015, **83**, 111, doi:10.1016/j.fct.2015.05.022.
2. Kumar G., Mittal S., Sak K., Tuli H. S., *Life Sci.*, 2016, **148**, 313, doi:10.1016/j.lfs.2016.02.022.
3. Luthra P. M., Lal N., *Eur. J. Med. Chem.*, 2016, **109**, 23, doi:10.1016/j.ejmech.2015.11.049.
4. Mehanny M., Hathout R. M., Geneidi A. S., Mansour S., *J. Controlled Release*, 2016, **225**, 1, doi:10.1016/j.jconrel.2016.01.018.
5. Ngo S. T., Li M. S., *Mol. Simul.*, 2013, **39**, 279, doi:10.1080/08927022.2012.718769.

6. Wright J. S., *J. Mol. Struct. THEOCHEM*, 2002, **591**, 207, doi:10.1016/S0166-1280(02)00242-7.
7. Ngo S. T., Li M. S., *J. Phys. Chem. B*, 2012, **116**, 10165, doi:10.1021/jp302506a.
8. Suhartanto H., Yanuar A., Hilman M. H., Wibisono A., Dermawan T., *Int. J. Comput. Sci. Issues*, 2012, **9**, 90.
9. Varghese M. K., *Molecular Dynamics Simulations of Some Nucleic Acids and Their Complexes*, Ph.D. Thesis, Mahatma Gandhi University, Kottayam, Kerala, India, 2009.
10. Wallace S. J., Kee T. W., Huang D. M., *J. Phys. Chem. B*, 2013, **117**, 12375, doi:10.1021/jp406125x.
11. Samanta S., Roccatano D., *J. Phys. Chem. B*, 2013, **117**, 3250, doi:10.1021/jp309476u.
12. Hazra M. K., Roy S., Bagchi B., *J. Chem. Phys.*, 2014, **141**, 18C501, doi:10.1063/1.4895539.
13. Yadav I. S., Nandekar P. P., Shrivastava S., Sangamwar A., Chaudhury A., Agarwal S. M., *Gene*, 2014, **539**, 82, doi:10.1016/j.gene.2014.01.056.
14. Parameswari A. R., Rajalakshmi G., Kumaradhas P., *Chem. Biol. Interact.*, 2015, **225**, 21, doi:10.1016/j.cbi.2014.09.011.
15. Priyadarsini K. I., *J. Photochem. Photobiol., C*, 2009, **10**, 81, doi:10.1016/j.jphotochemrev.2009.05.001.
16. Bonab M. I., Sardroodi J. J., Ebrahimzadeh A. R., Mehrnejad F., *J. Comput. Theor. Nanosci.*, 2015, **12**, 2077, doi:10.1166/jctn.2015.3988.
17. Dias Pereira C. I., Fabiano de Freitas C., Braga T. L., Braga G., Gonçalves R. S., Tessaro A. L., Graton Mikcha J. M., Hioka N., Caetano W., *Dyes Pigm.*, 2022, **197**, 109887, doi:10.1016/j.dyepig.2021.109887.
18. Jorgensen W. L., Maxwell D. S., Tirado-Rives J., *J. Am. Chem. Soc.*, 1996, **118**, 11225, doi:10.1021/ja9621760.
19. Ilnytskyi J., Patsahan T., Pizio O., *J. Mol. Liq.*, 2016, **223**, 707, doi:10.1016/j.molliq.2016.08.098.
20. Patsahan T., Ilnytskyi J., Pizio O., *Condens. Matter Phys.*, 2017, **20**, 23003, doi:10.5488/CMP.20.23003.
21. Van der Spoel D., Lindahl E., Hess B., Groenhof G., Mark A. E., Berendsen H. J. C., *J. Comput. Chem.*, 2005, **26**, 1701, doi:10.1002/jcc.20291.
22. Berendsen H. J. C., Grigera J. R., Straatsma T. P., *J. Phys. Chem.*, 1987, **91**, 6269, doi:10.1021/j100308a038.
23. Slabber C. A., Grimmer C. D., Robinson R. S., *J. Nat. Prod.*, 2016, **79**, 2726, doi:10.1021/acs.jnatprod.6b00726.
24. Kolev T. M., Velcheva E. A., Stamboliyska B. A., Spitteller M., *Int. J. Quantum Chem.*, 2005, **102**, 1069, doi:10.1002/qua.20469.
25. Humphrey W., Dalke A., Schulten K., *J. Mol. Graphics*, 1996, **14**, 33, doi:10.1016/0263-7855(96)00018-5.
26. Bachmann S. J., van Gunsteren W. F., *J. Phys. Chem. B*, 2014, **118**, 10175, doi:10.1021/jp5035695.
27. Woolley H. W., *J. Chem. Phys.*, 1953, **21**, 236, doi:10.1063/1.1698866.
28. Benjamin K. M., Schultz A. J., Kofke D. A., *Ind. Eng. Chem. Res.*, 2006, **45**, 5566, doi:10.1021/ie051160s.
29. Benjamin K. M., Schultz A. J., Kofke D. A., *J. Phys. Chem. C*, 2007, **111**, 16021, doi:10.1021/jp0743166.
30. Dezczyński M., Harding S. E., Winzor D. J., *Biophys. Chem.*, 2006, **120**, 106, doi:10.1016/j.bpc.2005.10.003.

Структурні аспекти кластерування молекул куркуміну в воді. Комп'ютерне моделювання методом молекулярної динаміки

Т. Пацаган¹, О. Пізіо²

¹ Інститут фізики конденсованих систем Національної академії наук України, вул. Свенціцького, 1, 79011 Львів, Україна

² Інститут Хімії, Національний автономний університет Мексики, м. Мехіко, Мексика

Ми досліджуємо кластерування молекул куркуміну у воді, використовуючи модель OPLS-UA для енольної форми куркуміну (J. Mol. Liq., **223**, 707, 2016) та модель SPC-E для води. З цією метою проведено комп'ютерне моделювання розчинів 2, 4, 8, 12, 16 та 20 молекул куркуміну в 3000 молекулах води із використанням методу молекулярної динаміки. Розраховано радіальні розподіли центрів мас молекул куркуміну та проаналізовано значення біжучих координаційних чисел. Прослідковано формування кластерів з часом. Отримано опис внутрішньої структури молекул у кластері за допомогою радіальних розподілів окремих елементів молекули куркуміну, орієнтаційних дескрипторів, параметра порядку та радіусу гірації. Розраховано коефіцієнт самодифузії кластерованих молекул куркуміну. Детально описано розподіл молекул води навколо кластерів. Виконано порівняння наших результатів з результатами комп'ютерного моделювання інших авторів. Обговорюється можливість зв'язку передбачень, отриманих для нашої моделі, та експериментально спостережуваних даних.

Ключові слова: куркумін, модель об'єднаних атомів, молекулярна динаміка, вода, кластери